ACS APPLIED MATERIALS & INTERFACES

Research Article

www.acsami.org

Multifunctional Electrochemical Platforms Based on the Michael Addition/Schiff Base Reaction of Polydopamine Modified Reduced Graphene Oxide: Construction and Application

Na Huang, Si Zhang, Liuqing Yang, Meiling Liu,* Haitao Li, Youyu Zhang,* and Shouzhuo Yao

Key Laboratory of Chemical Biology and Traditional Chinese Medicine Research (Ministry of Education), College of Chemistry and Chemical Engineering, Hunan Normal University, Changsha 410081, P. R. China

Supporting Information

ABSTRACT: In this paper, a new strategy for the construction of multifunctional electrochemical detection platforms based on the Michael addition/Schiff base reaction of polydopamine modified reduced graphene oxide was first proposed. Inspired by the mussel adhesion proteins, 3,4-dihydroxyphenylalanine (DA) was selected as a reducing agent to simultaneously reduce graphene oxide and self-polymerize to obtain the polydopamine-reduced graphene oxide (PDA-rGO). The PDA-rGO was then functionalized with thiols and amines by the reaction of thiol/amino groups with quinine groups of PDA-rGO via the Michael addition/Schiff base reaction. Several typical compounds containing thiol and/or amino groups such as 1-[(4-amino)phenylethynyl] ferrocene (Fc-NH_2), cysteine (cys), and glucose oxidase (GOx) were selected as the model molecules to anchor on the surface of PDA-rGO using the strategy for construction of multifunctional electrochemical platforms. The experiments revealed that the composite grafted with ferrocene derivative shows excellent catalysis activity toward many electroactive molecules and could be used for individual or simultaneous detection of dopamine hydrochloride (DA) and uric acid (UA), or hydroquinone (HQ) and catechol (CC), while, after grafting of cysteine on PDA-rGO, simultaneous discrimination detection of Pb^{2+} and Cd^{2+} was realized on the composite modified electrode. In addition, direct electron transfer of GOx can be observed when GOx-PDA-rGO was immobilized on glassy carbon electrode (GCE). When glucose was added into the system, the modified electrode showed excellent electric current response toward glucose. These results inferred that the proposed multifunctional electrochemical platforms could be simply, conveniently, and effectively regulated through changing the anchored recognition or reaction groups. This study would provide a versatile method to design more detection or biosensing platforms through a chemical reaction strategy in the future.

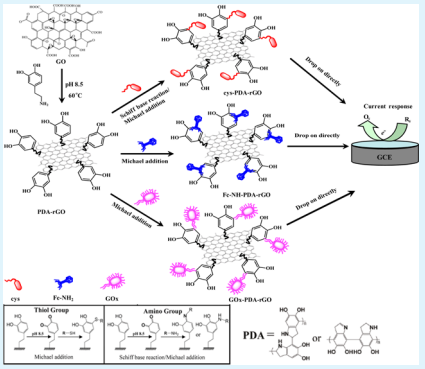

KEYWORDS: *multifunctional electrochemical platforms, polydopamine-reduced graphene oxide (PDA-rGO), Michael addition reaction/Schiff base reaction, catalysis, detection*

INTRODUCTION

The construction of multifunctional platforms has increased greatly in interest in recent years. It may be convenient to fabricate different sensors for different species simply through changing one recognition or reaction group of the multifunctional platforms. For this reason, much effort has been taken to develop novel materials for multifunctional platforms recently. For example, a multifunctional platform based on graphene oxide wrapped surface-enhanced Raman scattering (SERS) tags toward optical labeling and photothermal ablation of bacteria,[1] a multifunctional analytical platform on a paper strip for separation, preconcentration, and detection,[2] multifunctional nanoparticles and nanoshells for bioimaging and biosensing,[3,4] diagnosis and therapy of disease,[5] and multifunctional encoded self-assembling protein nanofibrils as a platform for multiplexed biomolecules detection have been reported recently.[6] These multifunctional platforms have been frequently employed in the biochemical areas for purposes such as detection of biomolecules and bioimaging based on the SERS,[2,6] plasmonic spectra, and fluorescence methods.[4]

However, it is difficult to establish multifunctional electrochemical platforms for the complicated modifying steps and hash preparation conditions. To our knowledge, there are many reports focusing on construction of a specific electrochemical biointerface for individual or multiple components detection. For example, biofunctionalized magnetic nanoparticles assemblies onto the graphene nanosheets have been used as immunosensing platform for simultaneous multiplexed electrochemical immunoassay using distinguishable signal tags.[7] Another multiplexed immunoassay platform for ultrasensitive and simultaneous detection of four biomarkers was developed on the basis of a hybridization chain reaction and biotin–

Received: May 28, 2015
Accepted: July 29, 2015
Published: July 29, 2015

DOI: 10.1021/acsami.5b04597
ACS Appl. Mater. Interfaces 2015, 7, 17935−17946

Scheme 1. Construction of the Multifunctional Electrochemical Detection Platforms Based on Michael Addition Reaction of PDA and Application in Detection of Electroactive Species

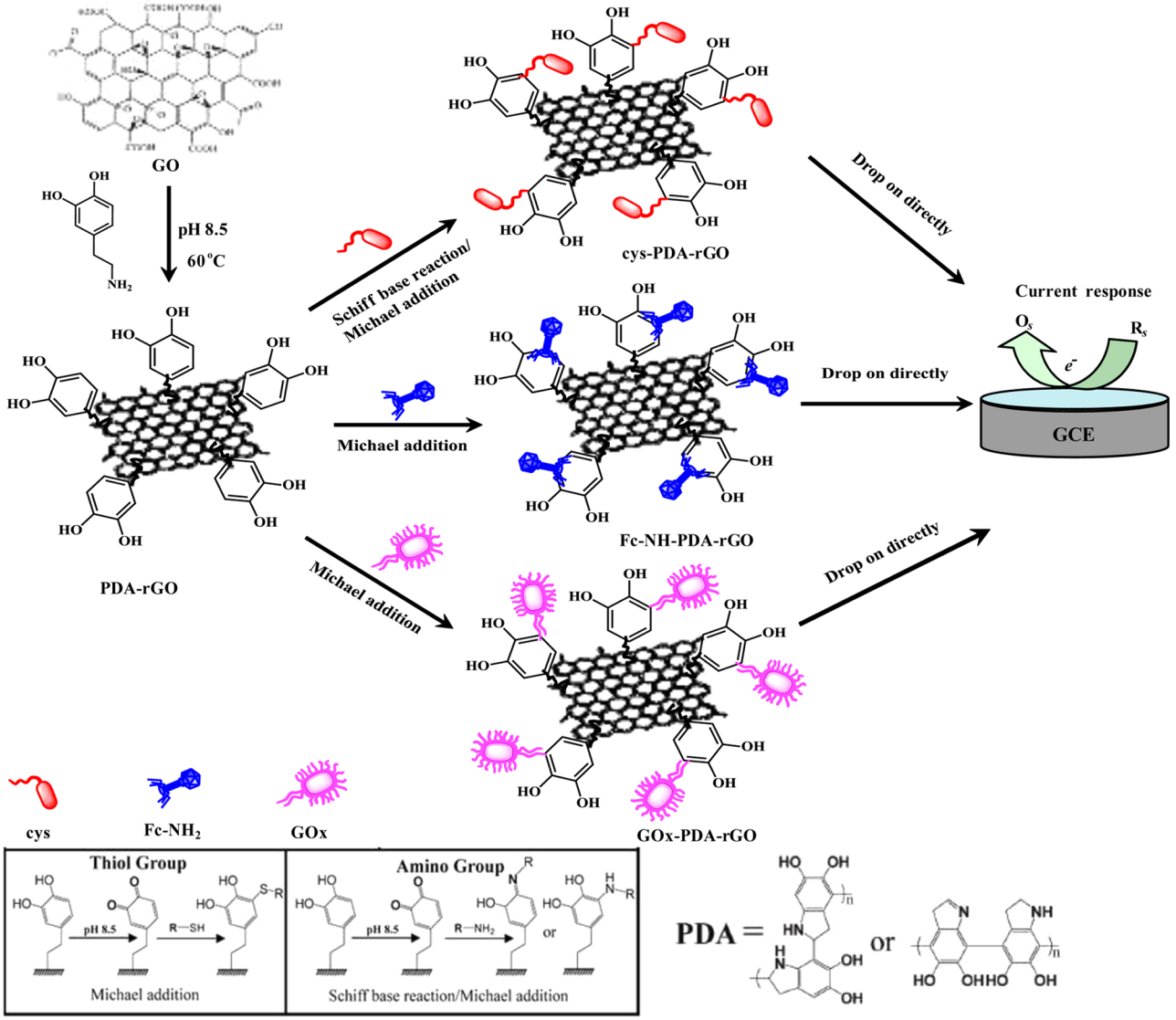

streptavidin signal amplification strategy.[8] It is proved that the magnetic nanoparticles and AuNPs used as the functional materials for immunosensing platforms are effective; however, the labeling process was complicated and the detected objects may be limited to biomarkers. Recently, Wu et al. developed a multifunctional electrochemical functionalization of an *N*-methyl-2-pyrrolidone-exfoliated graphene nanosheet (NMP-exfoliated GS) modified electrode as a highly sensitive analytical platform for phenols.[9] The NMP-exfoliated GS exhibited apparently better electrochemical activity toward the oxidation of a series of phenols, such as hydroquinone, catechol, 4-chlorophenol, and 4-nitrophenol. Apparently, this example is a successful electrochemical detection platform for multiple components. However, the platform cannot be tuned by changing the recognition or reaction group. Strictly speaking, it is a specific platform for multiplex detection, not a multifunctional platform for different purposes. Therefore, expanding the strategy for construction of multifunctional electrochemical platforms for detection and catalysis is of great significance.

It is considered that the key issue is to find an excellent electrode modification material for the multifunctional electrochemical platforms, which can be flexibly functionalized or grafted with different recognition molecules. In general, the materials used in the multifunctional electrochemical platforms should have good conductivity and stability, good adhesive property and compatibility, as well as enough functional groups for postlinking with different recognition groups to obtain multifunctional electrochemical platforms.

Mussel-inspired functional materials may be one of the best candidates, which have been widely implemented for various purposes, including modification and functionalizing of surfaces,[10−12] preparation of biomimetic functional materials,[13] immobilization of proteins,[14] enhancement of cell and hydroxyapatite adhesions,[15,16] enrichment and direct detection of small pollutant molecules,[17] severing as catalyst support and carbon adsorbent,[18,19] and synthesis of nanocubes.[20] The adhesive proteins of mussels, which contain high concentrations of catechol and amine functional groups, also exhibit excellent affinity for most organic and inorganic surfaces.[21] Inspired by the composition of adhesive proteins in mussels, the self-polymerization of DA (air-driven chemical polymerization of DA) has been used to prepare multifunctional

DOI: 10.1021/acsami.5b04597
ACS Appl. Mater. Interfaces 2015, 7, 17935−17946

biocompatible polydopamine (PDA) coatings on various surfaces for a variety of promising applications.[22] This self-polymerization reaction is so mild, without any complicated instruments and harsh reaction conditions.[23] During polymerization, PDA can spontaneously form a conformal and continuous coating layer on a wide variety of surfaces, including noble metals, metal oxides, synthetic polymers, semiconductors, and ceramics via the strong binding affinity of catechol functional groups. PDA can also serve as the linker to many materials to improve some critical performance of the initial materials, and/or to facilitate the covalent conjugation with moieties to possess other interesting functionalities. Interestingly, PDA can behave as both the reducing agent and stabilization agent for construction of several inorganic−organic hybrid materials.[24] It was reported that dopamine undergoes self-polymerization to produce an adherent of PDA, which allows dopamine to act simultaneously as a reducing agent for GO and as a capping agent to stabilize and decorate the resulting reduced GO (rGO) at weak alkaline pH media.[24]

The obtained PDA-rGO can be widely employed in many areas. A striking merit of the PDA-rGO is that the PDA layer on the surface of rGO is chemically active to various chemical molecules and hence can facilitate the design of various rGO-based hybrid materials. Therefore, the PDA-rGO demonstrates its prospect as a new platform of the surface chemistry.[10] For example, the synthesized PDA-rGO can be further functionalized by a chemical reaction strategy to obtain new platforms. To the best of our knowledge, a chemical reaction strategy, such as a "Click Chemistry" reaction, is an effective method to prepare the functional surfaces.[25−27] Similarly, the oxidized form quinone in PDA-rGO can undergo reactions with various functional groups, including thiols and amines via Michael addition or Schiff base reaction, to form covalently grafted functional layers. The reactions toward either amine- or thiol-containing molecules are facile, without any harsh reaction conditions or complicated equipment. More importantly, couplings with these nucleophiles typically proceed in aqueous environments and remain quite stable compared with those in the presence of nhydroxysuccinimide (NHS) or other cross-linkers. Several new materials, such as functional polymer brushes and [21] polymer hybrid materials based on the mussel-inspired chemistry, have been synthesized for improving the stability or dispersity of the initial polymers.[28] It is supposed that the "grafting-to" process may provide a versatile and benign means for the preparation of PDA-based materials. However, this method has seldom been employed in biosensing areas though there was no need of any additional cross-linkers when grafting thiol- and amine-containing molecules on the PDA modified surfaces. Up until now, construction of multifunctional platforms based on the PDA-rGO and thiol- or amine-containing molecules has not been reported yet.

Herein, considering the fascinating properties, such as reduction, self-polymerization of dopamine, and postgrafting property for PDA, a facile method for construction of multifunctional electrochemical platforms was reported based on the Michael addition or Schiff base reaction of PDA-rGO. Utilizing the mussel-inspired catecholamine reagent of dopamine, graphene oxide was reduced and functionalized simultaneously. Through the catechol functional group of PDA, several compounds containing thiol or/and amino groups (amine functional ferrocene derivative (Fc-NH_2), cysteine, glucose oxidase) were selected as the model molecules to anchor on the interface of PDA-rGO via Michael addition or Schiff base reaction (Scheme 1). By simply regulating the grafted functional molecules, the multifunctional detection platforms can be successfully fabricated and different electroactive species can be catalyzed and detected on the multifunctional electrochemical platforms, respectively.

EXPERIMENTAL SECTION

Reagents and Materials. Dopamine hydrochloride (DA), cysteine (cys), ascorbic acid (AA), uric acid (UA), hydroquinone (HQ), catechol (CC), acetaminophen (AC), glucose oxidase (GOx), and glucose were purchased from Sigma and used without further purification. 1-[(4-Amino) phenylethynyl] ferrocene (Fc-NH_2) was synthesized according to our published literature,[29] and the main synthesis procedures and characterization data were shown in the Supporting Information (S1). Graphene oxide (GO) was purchased from XFNANO Co., Ltd. (Nanjing, China) and used without further purification. All other chemicals were analytical grade and purchased from Sinopharm Chemical Reagent Co., Ltd. (Shanghai, China) and used directly. Ten millimolar of pH 8.5 Tris-HCl buffer solutions were used for PDA preparation and functionalization. Phosphate buffer solution (PBS, 0.1 M) was prepared with Na_2HPO_4, NaH_2PO_4, and 0.1 M Na_2SO_4. Acetate buffer solution (pH 4.5) was prepared with 0.1 mol L^{-1} HAc-NaAc aqueous solution. All aqueous solutions were prepared with Milli-Q ultrapure water.

Apparatus. A Varian-500 high resolution NMR spectrometer (Bruker AVANCE DRX500, Switzerland) and Thermo-Finnigan LCQ-advantage mass-spectrometer (GCMS-QP2010, Japan) were used to confirm the new compounds. The UV−vis spectra were obtained on a UV-2450 spectrophotometer (Shimadzu, Japan). FT-IR spectra were collected on a Nexus-670 Fourier transform-infrared spectrophotometer (Nicolet Instrument Co, USA) with the KBr pressed pellet transmission mode. Forty scans were averaged to yield the spectra with the resolution of 4 cm^{-1}. The field-emission scanning electron microscopy (FESEM) micrographs and energy dispersive X-ray spectroscopy (EDS) were obtained with SEM (Zeiss Sigma, Germany). For the SEM analysis, samples were prepared by dropping solution and drying on silicon wafers. X-ray photoelectron spectroscopy (XPS) measurements were carried out on K-Alpha 1063 (Thermo Fisher Scientific, England). Atomic force microscopy (AFM) images were revealed by a Multimode scanning probe microscopy (VEECO, USA). Electrochemical experiments, including cyclic voltammetry (CV), electrochemical impedance spectra (EIS), differential pulse voltammetry (DPV), square wave anodic stripping voltammetry (SWASV), were performed with a research electrochemical workstation of SP-150 (BioLogic Science Instruments, France) controlled by EC-Lab software. Glassy carbon electrode, saturated calomel electrode (SCE) and carbon rod electrode were served as work, reference and counter electrodes, respectively. All potentials here were cited versus the SCE. All experiments were performed at room temperature.

Synthesis of PDA-rGO. PDA-rGO was prepared typically as follows: 50 mg of GO and 50 mg of dopamine hydrochloride were added into 100 mL of 10 mM Tris-HCl solution (pH = 8.5) and dispersed by sonication for 10 min in an ice bath. The reaction mixture was stirred vigorously at 60 °C for 24 h. After the reduction reaction, PDA-rGO was filtered with a 0.2 μm membrane, filtered, centrifugated, washed, dispersed. The black powders were then filtrated and dried under reduced pressure for 24 h.

Surface Modification of PDA-rGO Based on Michael Addition/Schiff Base Reaction. Surface modification of PDA-rGO was performed by adding 10 mg of the PDA-rGO and 10 mg of Fc-NH_2 (or 10 mg of cysteine, or 10 mg of GOx) into 30 mL of 10 mM Tris-HCl solution (pH = 8.5). The reaction mixture was stirred at 35−40 °C for 24 h, and the as prepared composites were labeled as Fc-NH-PDA-rGO, cys-PDA-rGO, GOx-PDA-rGO. Possibly, owing to the bigger hindrance and the structure of Fc-NH_2, the reaction was slow. Therefore, in this case, small amount of MnO_2 was added in this system as the catalyst. After the reaction, the solution was filtered and

DOI: 10.1021/acsami.5b04597
ACS Appl. Mater. Interfaces 2015, 7, 17935−17946

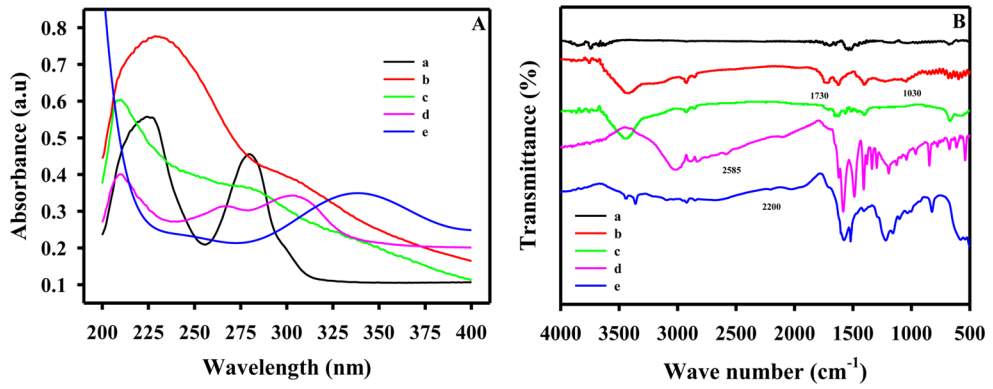

Figure 1. (A) UV spectra of DA (a), GO (b), PDA-rGO (c), Fc-NH_2 (d), Fc-NH-PDA-rGO (e). (B) FTIR spectra of DA (a), GO (b), PDA-rGO (c), cys-PDA-rGO (d), Fc-NH-PDA-rGO (e).

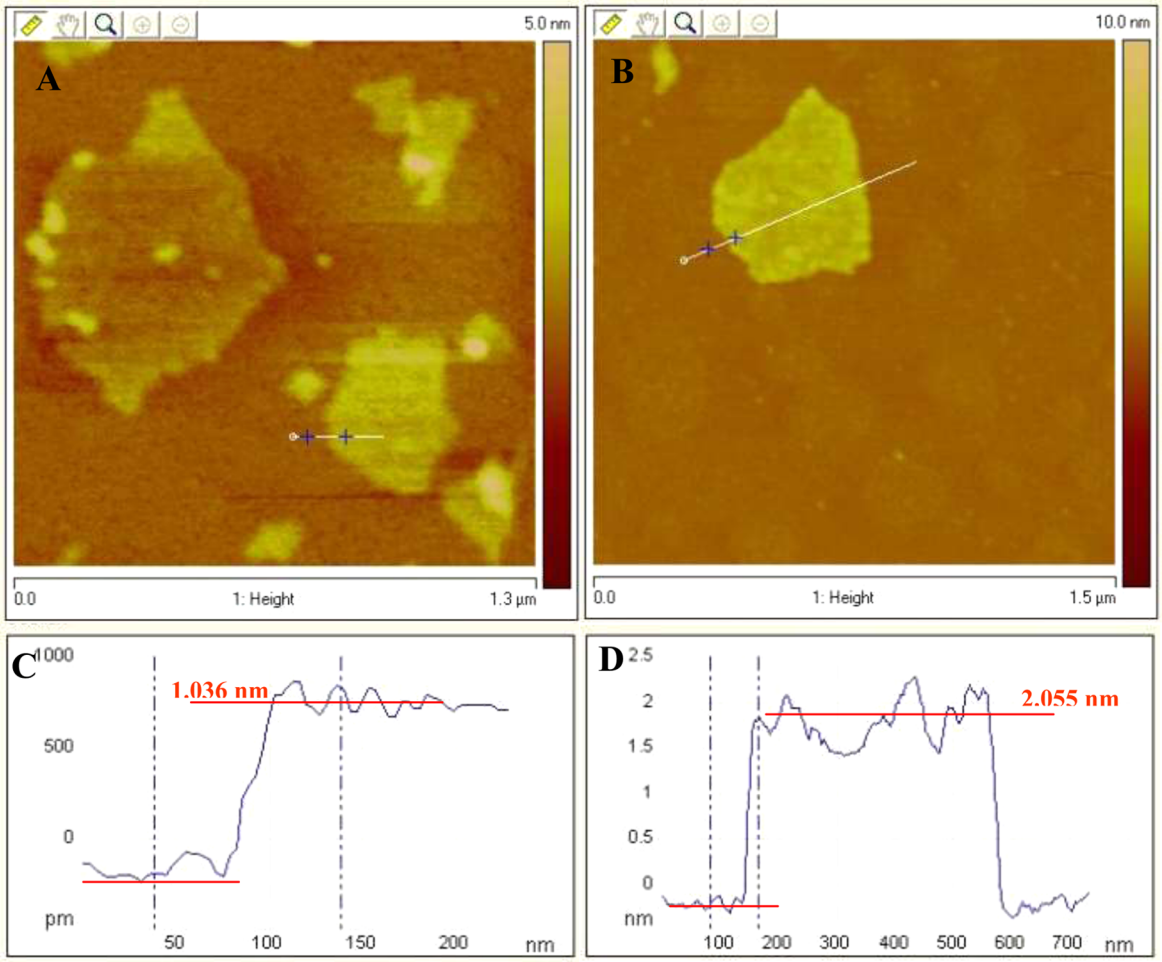

Figure 2. AFM images and height profile of GO (A, C) and PDA-rGO (B, D).

washed thoroughly with ultrapure water and ethanol, followed by drying under reduced pressure for further characterization.

Procedures for Catalysis or Detection of Electro-Active Molecules and Metal Ions Based on the Multifunctional Electrochemical Detection Platforms. After thoroughly characterization of PDA-rGO, Fc-NH-PDA-rGO, cys-PDA-rGO, GOx-PDA-rGO, the composites were used for construction of the electrochemical platforms. The GCE was successively polished with 1.0, 0.3, and 0.05 μm alumina powders, and then washed ultrasonically in ethanol and water alternately to obtain a mirror-like surface. The cleaned GCE was dried with nitrogen before modification. The composites of Fc-NH-PDA-rGO (1 mg mL^{-1}), cys-PDA-rGO (1 mg mL^{-1}) and GOx-PDA-rGO (1 mg mL^{-1}) were directly dropped onto the pretreated GCE. After dried in air, the modified GCE was stored at 4 °C under dry conditions when not in use. For comparison, PDA-rGO/GCE was also prepared using similar procedures.

RESULTS AND DISCUSSION

Construction of the Multifunctional Electrochemical Platforms and Its Possible Mechanism. When dopamine hydrochloride is added into an alkaline solution, the polymerization of dopamine monomers immediately occurs, coupled with the solution color change from colorless to pale brown,

DOI: 10.1021/acsami.5b04597
ACS Appl. Mater. Interfaces 2015, 7, 17935−17946

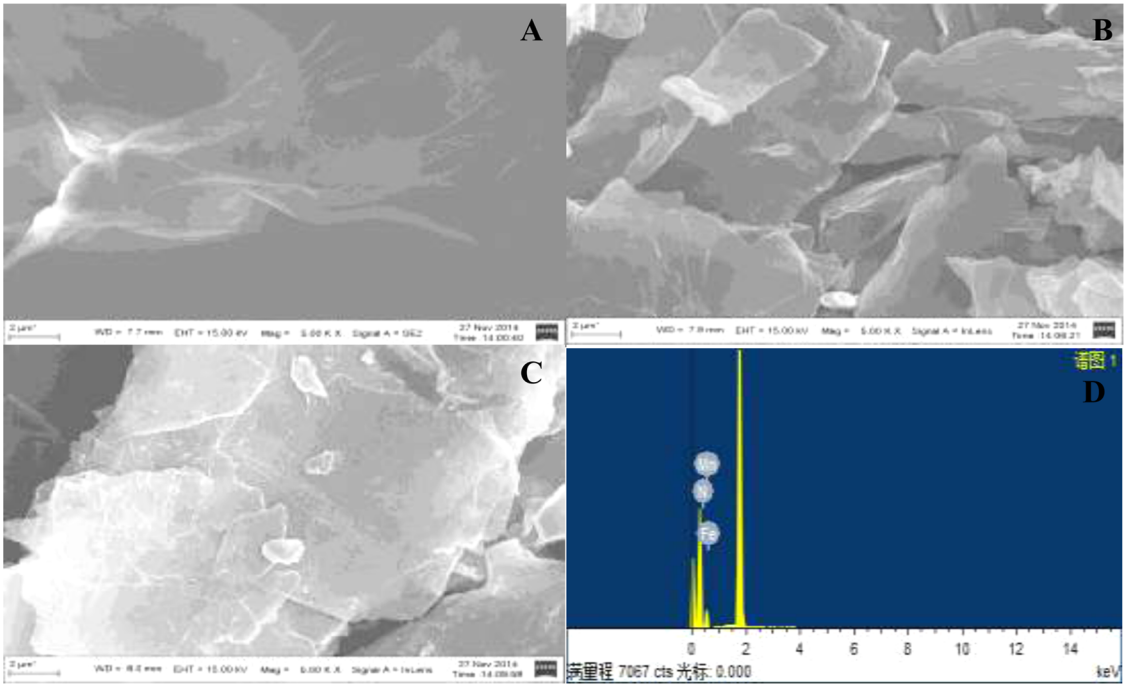

Figure 3. SEM images of GO (A), PDA-rGO (B), Fc-NH-PDA-rGO (C), and EDS of Fc-NH-PDA-rGO (D).

and finally to deep brown. In the presence of GO, dopamine undergoes self-polymerization to produce an adherent film of PDA and released electrons to reduce GO, which allows dopamine to simultaneously act as a reducing agent for GO and as a capping agent to stabilize and decorate the resulting rGO. The possible mechanism might be the released electrons during the polymerization of dopamine attacked the oxygen-containing species such as C═O in GO, and this electron transfer process seems to be the key procedure to complete reduction of GO.[24] Then, under the basic conditions, the catechol in the PDA matrix can be oxidized into the corresponding quinone, which can then react with the nucleophilic amine groups by means of Michael addition/Schiff base reaction.[30] Alternatively, this cross-linking reaction can proceed via a Michael-type addition pathway. In the case of thiol-contained molecules, the nucleophiles are most likely to react with PDA through Michael addition reaction. The reactions with either amine- or thiol-contained molecules are facile, without any harsh conditions or complicated procedures or equipment. More importantly, couplings with these nucleophiles typically proceed in aqueous environments and remain quite stable compared to *n*-hydroxysuccinimide (NHS) or maleimide agent commonly used as the coupling agents between the amine- or thiol-containing molecules and the substrate surfaces, which are susceptible to hydrolysis and thereby result in poor conjugation efficiency.[31] Therefore, choosing different molecules that contain amines or thiols to graft onto the PDA-rGO, the multifunctional electrochemical platforms can be obtained. In this paper, three typical amine- or thiol-contained molecules, such as cysteine, GOx, and Fc-NH_2 were selected as typical molecules to anchor on the surface of PDA-rGO for constructing the multifunctional electrochemical platforms (Scheme 1). The successful functionalization and grafting processes were confirmed by IR, UV, XPS, and electrochemical methods, and the Results and Discussion are displayed below.

Characterization of the PDA-rGO Composite and Multifunctional Electrochemical Platforms. *Characterization of the PDA-rGO.* PDA-capped rGO was prepared via simultaneous reduction of GO by dopamine and self-polymerization of dopamine in Tris-HCl. The process can be confirmed by UV−vis absorption and IR spectroscopy. In Figure 1A, the characteristic absorbance peaks for GO (b) at 230 and 300 nm shifted to 210 and 280 nm (c) in PDA-rGO. And the intensity of the absorbance peaks increased with the reduction time (Supporting Information, Figure S1). The PDA-rGO remains uniformly dispersed in Tris-HCl. Thus, GO has been reduced and the aromatic structure within the GO nanosheets restored upon dopamine reduction.[21] These results can be further confirmed by IR. As shown in Figure 1B (c), after reaction with dopamine, the band at 1730 cm^{-1} for the carbonyl group almost disappeared,[10] indicating that GO was reduced and the rGO was obtained. The peaks at 1519 cm^{-1} (−NH_2 scissoring vibration) and 1342 cm^{-1} (−CH_2 bending vibration) are observed in the spectrum of PDA-rGO. The band at 3420 cm^{-1} can be ascribed to the − NH group of PDA, showing that dopamine was self-polymerized and PDA-rGO was formed.[24]

In order to further confirm the reduction of GO and functionalization of PDA on rGO, AFM was conducted. Figure 2 shows the morphology and thickness of GO and PDA-rGO. The thickness of GO sheets was around 1.036 nm (Figures 2A and C), which is thicker than pristine graphene.[32] On the other hand, the average thickness of PDA-rGO was around 2.055 nm (Figures 2B and D), indicating that the increase in thickness of 1.019 nm is due to the presence of PDA on the rGO sheets.[33]

Characterization of the Multifunctional Electrochemical Platforms. Three typical amine- or thiol-containing molecules, cysteine, GOx, and Fc-NH_2 were selected to graft onto the PDA-rGO to construct the multifunctional electrochemical platforms. As shown in Figure 1B (d), after reaction with cysteine, the characteristic band of −SH at 2585 cm^{-1} was clearly observed in the IR spectrum. Therefore, the main reaction site for cysteine might be the −NH_2 group, and a large amount of −SH still remained in the resultant composite. The possible mechanism and products are shown in the Supporting

DOI: 10.1021/acsami.5b04597
ACS Appl. Mater. Interfaces 2015, 7, 17935−17946

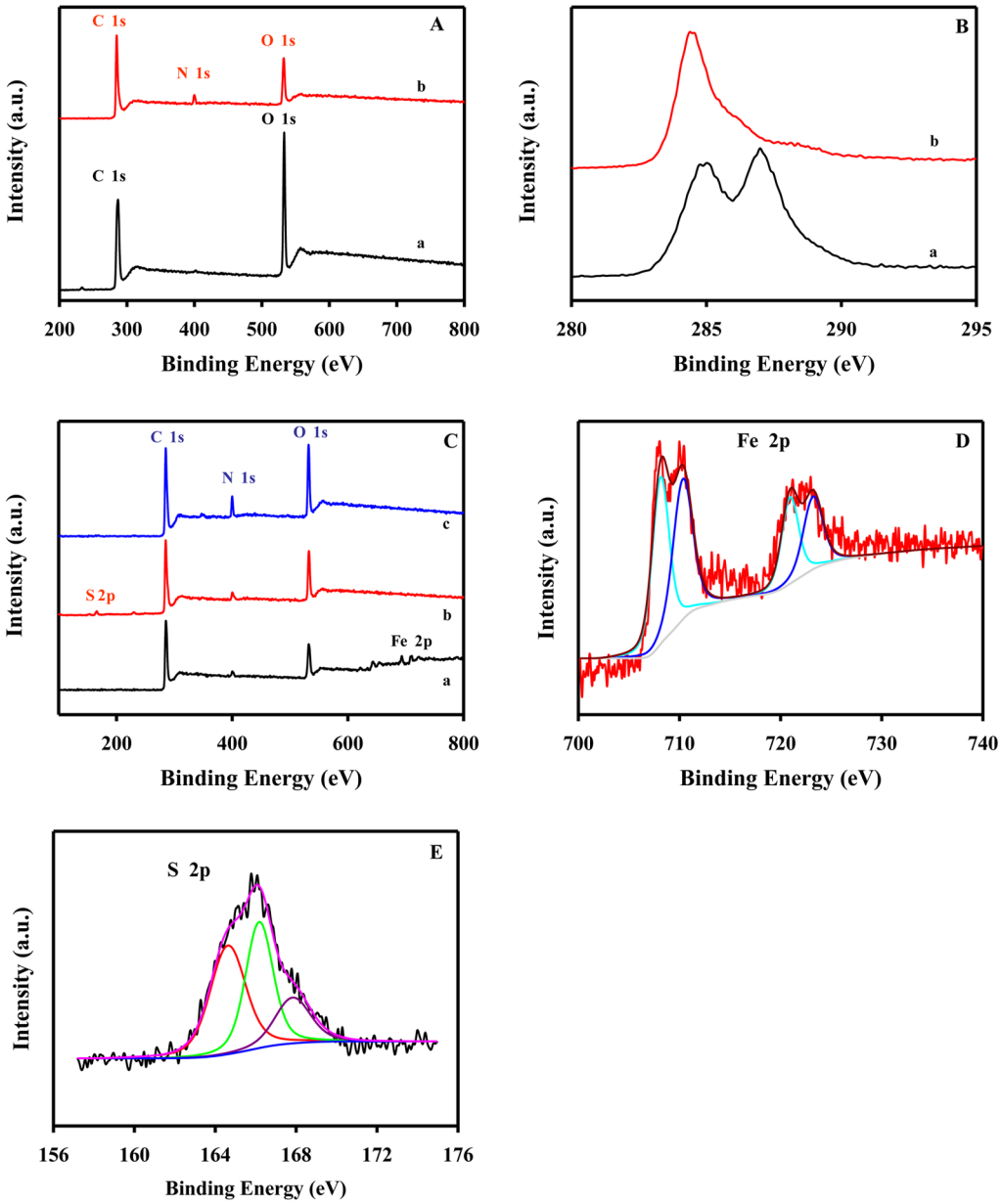

Figure 4. XPS survey spectra (A) of GO (A-a) and PDA-rGO (A-b), Fc-NH-PDA-rGO (C-a), cys-PDA-rGO (C-b), and GOx-PDA-rGO (C-c), and the C 1s binding energy regions of GO (B-a) and PDA-rGO (B-b), (D) Fe 2p, and the (E) S 2p region.

Information (Scheme S1). This indicated that the reaction of cysteine with PDA-rGO was relatively easier. However, for the grafting of the ferrocene derivative, the reaction is relatively slow. The reasons may be as follows: First, the Fc-NH_2 contains a benzene ring which was conjugated with the $-NH_2$ owing to the p-π conjugation relation. This will reduce the nucleophilicity of Fc-NH_2, and the resulting reactivity of the aromatic amine was smaller than that of the aliphatic amine. Second, the acetenyl is an electron deficiency group under basic conditions, and this will decrease the alkalinity of the aromatic amine, which will also result in the decreasing of reaction activity. Therefore, in this case, a small amount of catalyst MnO_2 was added. After grafting of Fc-NH_2, the maximum absorbance peaks at 280 nm in Figure 1A (c) notably shifted to 338 nm in Figure 1A (e), as shown in the UV spectra. In the IR spectrum of ferrocene derivative modified PDA-rGO in Figure 1B (e), the characteristic peaks at 2200 cm^{-1} for C≡C, 799 cm^{-1} for ferrocene, and 3420 cm^{-1} for − NH were found. Therefore, the ferrocene derivative was successfully grafted onto the PDA-rGO via Michael addition through reaction of $-NH_2$ and quinone groups. As shown in Figure S2 in the Supporting Information, the native GOx molecule (Figure S2, a) displays three distinct peaks located at 1652, 1571, and 1052 cm^{-1}, which correspond to the amide I and amide II absorption band and the C−O bond stretching vibration of GOx, respectively.[34] The typical IR spectra for the GOx grafted composite also exhibited these two typical amide I and amide II absorption bands (Figure S2, c) at 1657 and 1571 cm^{-1}, which were almost the same as those of the native GOx (Figure S2, a). The slight shifts of amide I and II absorption bands may result from the interaction between GOx and PDA-rGO.[35] It is generally accepted that the disappearance of the amide II band is responsible for the unfolding and denaturation of the immobilized enzymes.[35] In this study, the existence of the amide II absorption band

DOI: 10.1021/acsami.5b04597
ACS Appl. Mater. Interfaces 2015, 7, 17935−17946

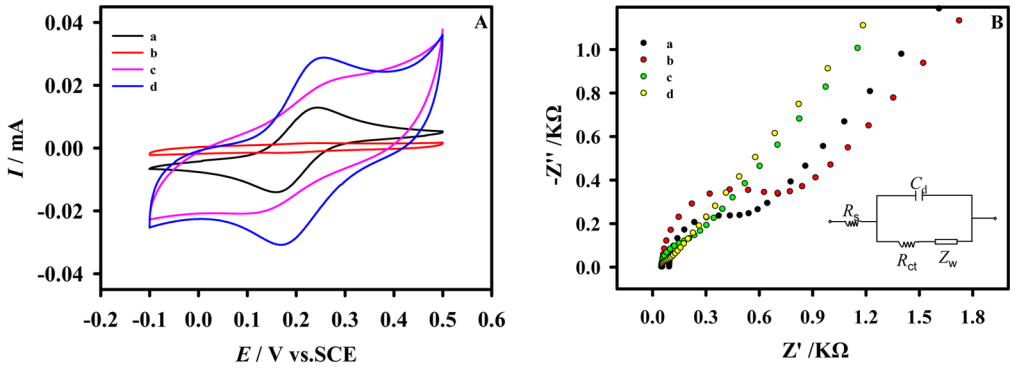

Figure 5. CVs (A) and EIS (B) of bare GCE (a), GO/GCE (b), PDA-rGO/GCE (c), and Fc-NH-PDA-rGO/GCE (d) in 2 mM $Fe(CN)_6^{3-/4-}$ containing 0.1 M Na_2SO_4.

demonstrated that GOx was grafted onto the PDA-rGO film and remained near their native states, and the PDA-rGO composite displayed good biocompatibility and strong affinity to GOx. Therefore, through Schiff-base reaction or Michael addition reaction, the "grafting-to" process was successfully realized.

The successful functionalization of PDA and the postgrafting of functional molecules can be further confirmed by SEM and XPS. The typical SEM photos of GO/GCE, PDA-rGO/GCE, and Fc-NH-PDA-rGO/GCE are shown in Figures 3, which provided further evidence for the successful attachment of PDA and grafting of Fc-NH_2. The GO shows an obvious conglomeration surface with cracks and wrinkles. After modification with PDA and reduction, the surface of GO became rougher, and this suggested that PDA was coated on the rGO. When grafted with Fc-NH_2, there were several small particles decorated on the surface of PDA-rGO, which may be the MnO_2 or Fc-NH_2 dispersed on the surface. Energy dispersive X-ray spectroscopy (EDS) was used to analyze the chemical composition of PDA-rGO after the attachment of Fc-NH_2, and it was found that the peak of Fe and Mn was obviously found as shown in Figure 3D. Therefore, when grafting of Fc-NH_2 on the PDA-rGO, a small amount of MnO_2 was doped into or remained in the composite at the same time. It is reported that MnO_2 is a good catalyst and excellent material which can be used for determination of some electroactive molecules when combining with graphene oxide.[36] Owing to the fact that the removal of MnO_2 is complicated, and considering the special property of it, the resultant Fc-NH-PDA-rGO was used directly. Therefore, MnO_2 in the system may not only act as a catalyst for the Michael addition reaction, but also increase the catalysis property of the Fc-NH-PDA-rGO.

The PDA coating on the rGO sheets was also proved by XPS. XPS survey spectra of GO and PDA-rGO samples in Figure 4A showed that an N 1s peak at 398 eV was observed only in the PDA-rGO sample. The N 1s peak originates from the amine groups of the PDA on rGO. From the XPS spectrum of the PDA-rGO sample, the nitrogen/carbon atomic ratio (N/C) was calculated to be 0.062 (Table S1, Supporting Information). It has been reported that the theoretical value of N/C in dopamine is 0.125 and the N/C value in PDA layers on different substrates is between 0.1 and 0.13.[23] So, if we consider the rGO layer as a substrate, the N/C value of 0.062 in our sample is quite reasonable. Figure 4B shows that, in the C 1s binding region, a peak due to oxygen-containing groups between 286 and 290 eV in the GO sample has been mostly removed in the PDA-rGO sample, indicating partial reduction of GO by the polymerization of dopamine.[33] After grafting of three typical amine or thiol-contained molecules, the characteristic peaks of S, N, or Fe were increased or changed obviously. In the survey spectra of Fc-NH-PDA-rGO and cys-PDA-rGO composite, the atom contents for Fe and S were 1.41 and 1.83 (Figure 4C–E, Table S1), and these results indicated that Fc-NH_2 and cysteine were grafted onto the PDA-rGO. For the GOx anchored composite, the atom contents of O and N increased, which may result from grafting of GOx.

The $Fe(CN)_6^{3-/4-}$, as an electrochemical probe, is usually used to evaluate the electrochemical properties of the electrode. Figure 5A shows the CV obtained at the bare GCE (a), GO/GCE (b), PDA-rGO/GCE (c), and Fc-NH-PDA-rGO/GCE (d) in 2 mM $Fe(CN)_6^{3-/4-}$ solution containing 0.1 M Na_2SO_4. It is noted that the potentials between the anodic and cathodic peaks (ΔE_p) are different for these electrodes. As ΔE_p is a function of the electron transfer rate, the lower the ΔE_p, the higher the electron transfer rate. The order of ΔE_p values at different electrodes is as follows: Fc-NH-PDA-rGO < PDA-rGO < GCE < GO/GCE. Furthermore, the redox peak currents at the Fc-NH-PDA-rGO/GCE are larger than those of the PDA-rGO/GCE and GCE. This may result from the good electronic conductivity and large specific surface area of Fc-NH-PDA-rGO/GCE. The smaller ΔE_p and the higher redox peak currents at Fc-NH-PDA-rGO/GCE indicated that this electrode had better electrochemical properties than those of the PDA-rGO/GCE and GCE.

The electron transfer properties of the different electrodes were further characterized by EIS. Figure 5B presents the Nyquist plots of GCE (a), GO/GCE (b), PDA-rGO/GCE (c), and Fc-NH-PDA-rGO/GCE (d). The Nyquist plots were fitted by the Randles equivalent circuit (Figure 5B, inset). The Nyquist plot has taken into consideration the diffusion and kinetic controlled parameters. The Randles equivalent circuit used for fitting the impedance data consists of the solution resistance (R_s) connected in series to the parallel combination of the capacitance (C_d), charge transfer resistance (R_{ct}), and Warburg impedance (Z_W). The R_{ct} of the electrode is equal to the semicircle diameter of the Nyquist diagram. Well-defined semicircles with R_{ct} of 280 Ω and 480 Ω at higher frequencies were obtained for the bare GCE and GO/GCE (Figure 5B, a and b), indicating that relatively larger interface electron transfer resistances were obtained at these two electrodes. When PDA-rGO/GCE was conducted (Figure 5B, c), the diameter of the semicircle in the high frequency region was decreased to 110 Ω, which suggested that PDA-rGO could

DOI: 10.1021/acsami.5b04597
ACS Appl. Mater. Interfaces 2015, 7, 17935–17946

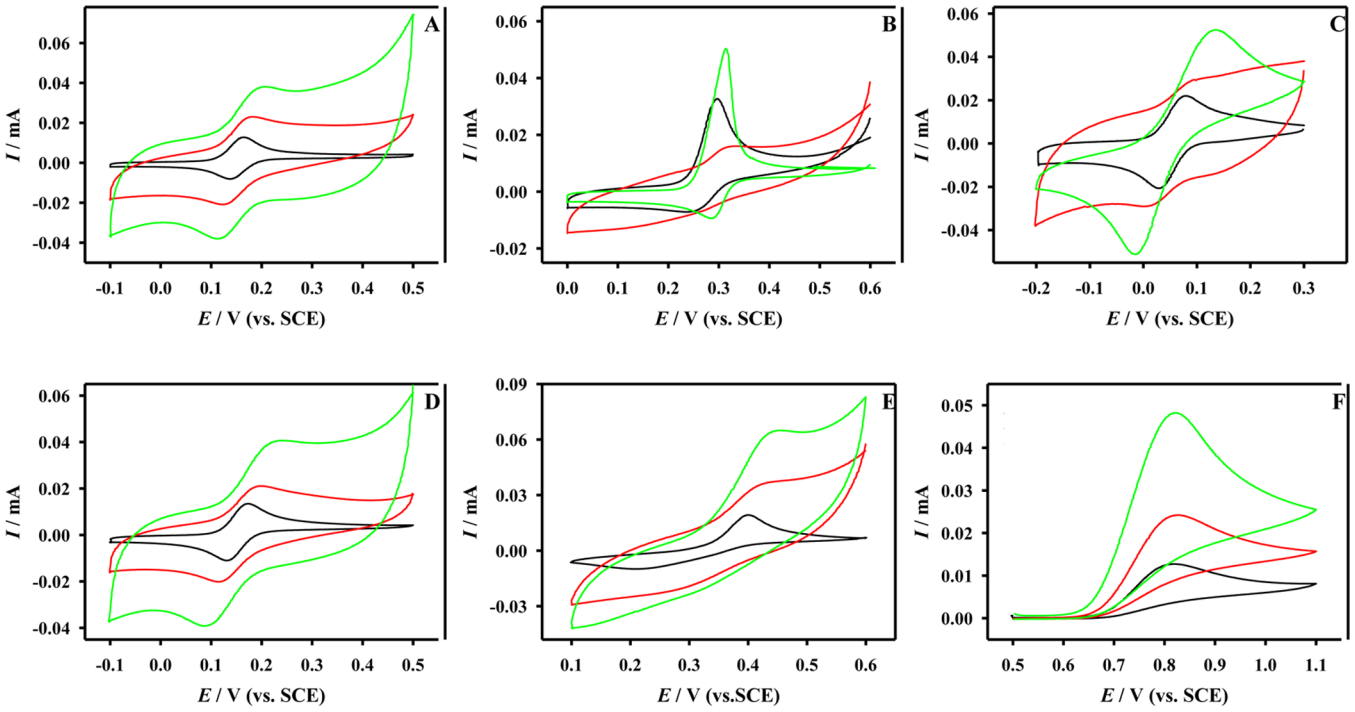

Figure 6. CVs of bare GCE (black curve, a), PDA-rGO/GCE (red curve, b), and Fc-NH-PDA-rGO/GCE (green curve, c) in buffer solution (pH 7) containing DA (A), UA (B), HQ (C), CC (D), AC (E), and $NaNO_2$ (F) . Concentration: 10 μM; scan rate: 50 mV/s.

improve the conductivity and accelerate the electron transfer speed. For the Fc-NH-PDA-rGO/GCE (Figure 5B, d), the R_{ct} value further decreased to 25 Ω. Therefore, the conductivity was obviously improved on the Fc-NH-PDA-rGO/GCE, which agreed with the CV results. Similarly, the CV and EIS of GOx-PDA-rGO/GCE (Figure S3, Supporting Information) and cys-PDA-rGO/GCE (Figure S4, Supporting Information) were also compared with PDA-rGO, GO/GCE, and GCE. The CV and EIS results indicated that the GOx and the cysteine were successfully anchored on PDA-rGO, and the conductivity was much better than others.

Application of the Multifunctional Electrochemical Platforms. *Application of the Functional Platform of Fc-NH-PDA-rGO/GCE.* Some electroactive molecules were selected as the models to investigate the electrocatalysis property of the Fc-NH-PDA-rGO/GCE, as shown in Figure 6. It was found that DA (A), UA (B), HQ (C), CC (D), AC (E), and $NaNO_2$ (F) can be easily oxidized on the Fc-NH-PDA-rGO/GCE (c), and much larger oxidation currents can be obtained compared with GCE (a) and PDA-rGO/GCE (b). The reasons may result from the catalysis of the Fc-NH-PDA-rGO composite. First, PDA is a conductive polymer and the rGO-PDA has large surface area and good conductivity property. Furthermore, the electron transfer speed further accelerated after grafting of the ferrocene derivative electron mediator. Therefore, the synergetic catalysis effect of PDA-rGO and ferrocene derivative make the oxidation peak current enhanced on the Fc-NH-PDA-rGO/GCE.

Another application of the Fc-NH-PDA-rGO/GCE platform is detection of some specific electroactive molecules or simultaneous detection of two species in the complex samples. The selective detection of neurotransmitters is of substantial interest for the rapid and early detection of neural disorders. Therefore, owing to the different oxidation peak potentials for DA and UA on the Fc-NH-PDA-rGO/GCE in Figure 6, the determination of DA and UA is selected as a model system. As shown in Figures S5A and B in the Supporting Information, the individual detection of DA or UA was conducted. It was shown that, in a wide detection range, the peak currents increased with the concentrations of DA or UA, and the detection limits can be calculated as 0.025 and 0.06 μM, respectively. Considering the coexistence of DA, AA, and UA in real biological samples, the selective detection of DA and UA was then investigated accordingly in the triplex solution. Figures 7A and B show the responses of the Fc-NH-PDA-rGO/GCE upon addition of different concentrations of DA or UA with the coexistence of fixed concentrations of the other two species. The peak potentials are located at 0.15 and 0.31 V, respectively, which are well separated from each other. The peak currents of DA and UA increased with their concentrations, while the peak of AA did not appear.

As the concentrations of DA and UA increased simultaneously as shown in Figure 7C, the characteristic oxidation peak currents of them increased accordingly. The calibration curve corresponding to the oxidation peak currents of DA and UA at variable concentrations is depicted in the inset plots. The detection ranges and detection limits for DA and UA are 0.03 and 0.07 μM in Figure 7C, which were summarized in Table S2 in the Supporting Information. In order to estimate its performance, the sensitivity was calculated according to the slope of the calibration curve,[37] given the results of 260 and 152 μA L μg^{-1} cm^{-2} for DA and UA, respectively. The platform was also compared with those of the counterparts reported in the literature, and the results are shown in Table S3 in the Supporting Information.

Furthermore, similar results were obtained for detection of HQ and CC. Figures S6A and B in the Supporting Information show the detection of HQ and CC in the individual samples, respectively. It is shown that the peak currents increased with the concentrations of HQ and CC. In Figures 7D and E, for the

DOI: 10.1021/acsami.5b04597
ACS Appl. Mater. Interfaces 2015, 7, 17935−17946

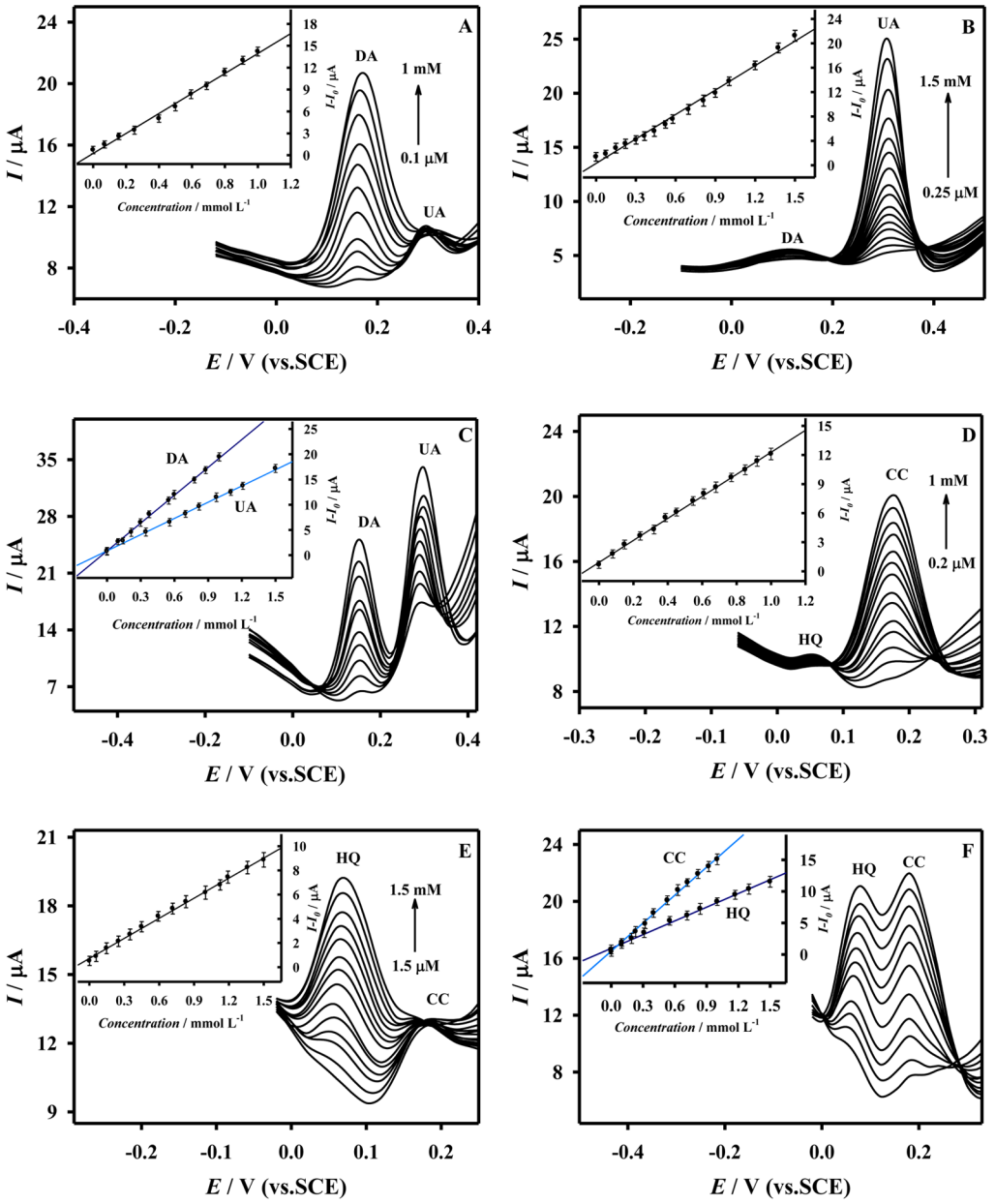

Figure 7. DPVs of Fc-NH-PDA-rGO/GCE in mixtures of (A–C) DA, UA, and AA and of (D–F) CC and HQ in 0.1 M PBS (pH 7). Concentrations: (A) DA ranging from 0.1 μM to 1 mM in the presence of 300 μM AA and 30 μM UA; (B) UA ranging from 0.25 μM to 1.5 mM in the presence of 300 μM AA and 30 μM DA; (C) Various concentrations of DA and UA in the presence of 300 μM AA in PBS. (D) CC with concentrations from 0.2 μM to 1 mM in the presence of 30 μM HQ; (E) HQ with concentrations from 1.5 μM to 1.5 mM in the presence of 30 μM CC; (F) Various concentrations of HQ and CC in PBS. Inset: the relationship between the peak currents and concentrations.

individual analysis of CC and HQ on the Fc-NH-PDA-rGO/GCE in the two-component system, they can be well separated with the ΔE_p of 120 mV and the peak currents were linear relative to their concentrations. The respective calibration curves for the DPV are depicted in the inset plots of Figures 7D and E.

As the concentrations of HQ and CC increased simultaneously, as shown in Figure 7F, the characteristic oxidation peak currents increased accordingly. The detection limits for HQ and CC were 0.3 and 0.07 μM with simultaneous determination of the two species. According to the slop of the calibration curves, the sensitivity can be calculated to be 103 and 209 μA L μg^{-1} cm^{-2} for HQ and CC, respectively. The linear range and determination limit of this sensor were also compared with those in the literature, as shown in Table S4 in the Supporting Information. The results indicated that the platform was better or the same as many of the reported sensors.

Application of the Functional Platform of cys-PDA-rGO/GCE. A sensitive platform for the simultaneous electrochemical determination of Cd^{2+} and Pb^{2+} in aqueous solution has been developed based on the cys-PDA-rGO/GCE. Figure 8A shows the SWASV curves of GCE (a), PDA-rGO/GCE (b), and cys-PDA-rGO/GCE (c) by in situ plating bismuth film for Cd^{2+} and Pb^{2+} determination. The detection was conducted in the media of 0.1 M of pH 4.5 acetate buffered saline containing 20 $\mu g\ L^{-1}$ Cd^{2+}, 20 $\mu g\ L^{-1}$ Pb^{2+}, and 400 $\mu g\ L^{-1}$ Bi^{3+}. The anodic stripping peaks of Cd^{2+} at −0.76 V and Pb^{2+} at −0.52 V were

DOI: 10.1021/acsami.5b04597
ACS Appl. Mater. Interfaces 2015, 7, 17935−17946

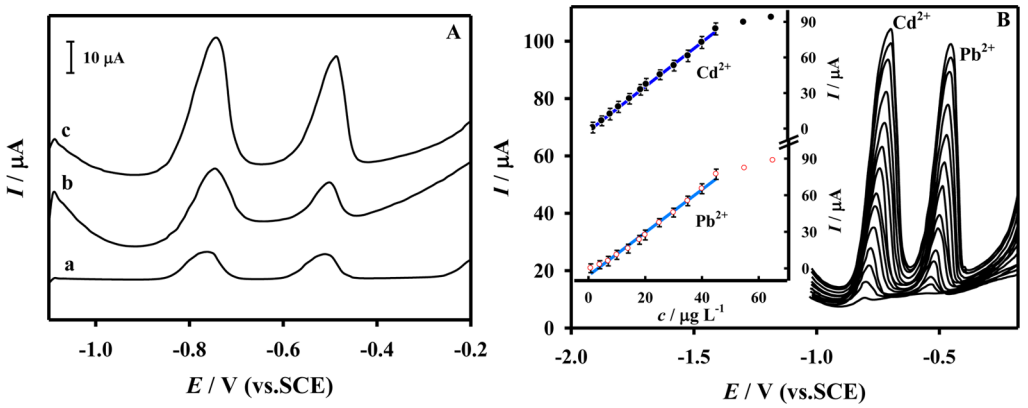

Figure 8. (A) SWASV curves of 20 μg L^{-1} of Cd^{2+} and Pb^{2+} at Bi/GCE (a), Bi/PDA-rGO/GCE (b), and Bi/cys-PDA-rGO/GCE (c). (B) SWASV and calibration (inset) curves on Bi/cys-PDA-rGO/GCE for Cd^{2+} and Pb^{2+} at different concentrations. SWASV conditions: acetate buffer (pH 4.5) containing 400 μg L^{-1} Bi^{3+}, deposition potential at −1.1 V, deposition time of 400 s, amplitude of 0.025 V, increment potential of 0.004 V, and pulse period of 0.2 s.

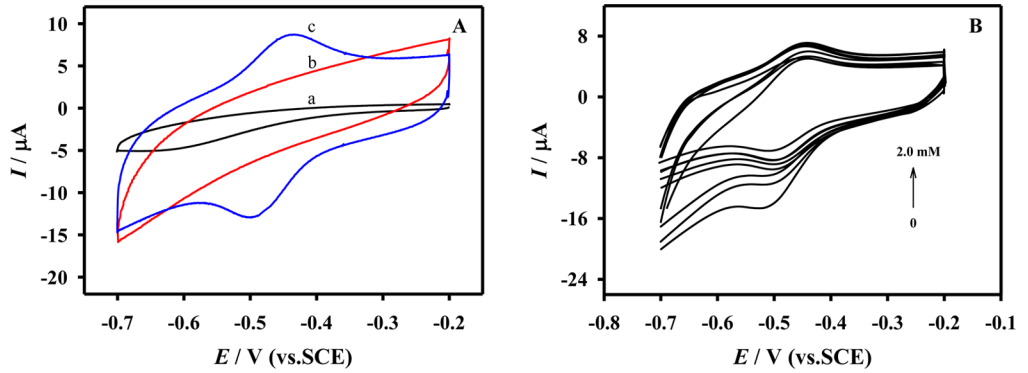

Figure 9. (A) CVs of bare GCE (a), PDA-rGO/GCE (b), and GOx-PDA-rGO/GCE/GCE (c) in N_2 saturated 0.1 M PBS (pH 7.4) in the absence of glucose at a scan rate of 400 mV s^{-1}; (B) CV responses of GOx-PDA-rGO/GCE with different concentrations of glucose in air-saturated 0.1 M PBS (pH 7.4).

presented in the bismuth film-modified GCE. The peak potentials of Cd^{2+} and Pb^{2+} positively shifted on the bismuth film-modified PDA-rGO/GCE. In the meantime, the peak potentials of Cd^{2+} and Pb^{2+} on the cys-PDA-rGO/GCE further positively shifted and took 191% and 137% peak height enhancement compared with that of GCE. The main reasons for the amplifying effect were as follows: The thiol groups maintained their original state after grafting onto the PDA-rGO, which can coordinate with Cd^{2+} and Pb^{2+} to collect the metal ion and enhance the sensitivity. On the other hand, the enlarged, activated surface and good electrical conductivity of PDA-rGO contributed to the collection and deposition of Cd^{2+} and Pb^{2+} on the electrode surface. The synergistic coordination effect of cysteine as well as the enrichment effect of PDA-rGO makes the cys-PDA-rGO/GCE show good performance upon detection of ions. Under the optimal conditions (Figure S7, Supporting Information), the simultaneous analysis of Cd^{2+} and Pb^{2+} was performed on the Bi/cys-PDA-rGO/GCE with increasing metal ion concentrations from 0.40 μg L^{-1} to 80 μg L^{-1}, as shown in Figure 8B. The linear relationship existed between the currents and the concentrations of Cd^{2+} and Pb^{2+} in the range of 0.40 μg L^{-1} to 45 μg L^{-1} with the detection limits of 0.10 μg L^{-1} for Cd^{2+} and 0.12 μg L^{-1} for Pb^{2+}, respectively, based on the signal-to-noise ratio of 3 (S/N = 3). The sensor shows good sensitivity, and the linear range and determination limit of this sensor are better or the same as those listed in the literature (Table S5, Supporting Information).

Application of the Functional Platform of GOx-PDA-rGO/GCE. As shown in the Supporting Information (Figure S2), after being grafted onto the PDA-rGO, the amide I and amide II peaks of GOx were observed in the IR spectra of GOx-PDA-rGO/GCE, confirming that the GOx was effectively grafted onto the PDA-rGO surface and retained its native states. The direct electron transfer behavior of GOx-PDA-rGO/GCE was investigated by CV. Figure 9A shows the CVs of bare GCE (a), PDA-rGO/GCE (b), and GOx-PDA-rGO/GCE (c) in N_2-saturated PBS. A pair of distinct and nearly symmetric redox peaks was observed at the GOx-PDA-rGO/GCE (c), which could be originated from the electron transfer between GOx and the underlying electrode. The formal potential is −0.468 V, which is in good agreement with the previously published data for the $FAD/FADH_2$ redox center of GOx in a neutral solution.[34,38] The oxidation of peak current increased with the scan rate, as shown in Figure S8, which means that the oxidation is a mass-transfer controlled process. Therefore, the PDA-rGO could provide a biocompatible and conductive microenvironment which can promote direct electron transfer between GOx and GCE with the aid of PDA-rGO. The direct bioactivity of the immobilized GOx to glucose was investigated and characterized by CVs at the GOx-PDA-rGO/GCE in the air-saturated PBS. As depicted in Figure 9B, when glucose was added, the shape of the CVs of the GOx-PDA-rGO/GCE

DOI: 10.1021/acsami.5b04597
ACS Appl. Mater. Interfaces 2015, 7, 17935−17946

changed and an obvious decrease in the reduction peak current can be found. The larger the amount of glucose was added, the smaller the reduction current obtained, indicating the consumption of oxygen. Based on this phenomenon, the concentration of glucose may be determined on the GOx-PDA-rGO modified electrode.

CONCLUSION

In summary, a new strategy for construction of multifunctional electrochemical platforms by grafting of thiols and amines on the PDA modified reduced graphene oxide via Michael addition/Schiff base reaction was developed. The multifunctional electrochemical platforms can be easily obtained by simply changing the grafted molecules on the PDA-rGO. When casting the as prepared composites on an electrode, multifunctional electrochemical platforms can be fabricated for direct catalysis or determination of some electro-active species. The method will also allow anchoring other thiol- or amino-functionalized molecules, polymers, and proteins, thus providing a versatile means for the preparation of multifunctional graphene-based materials and sensors. This stepwise chemical reaction strategy can also provide a powerful tool to design biosensing approaches for the highly selective detection aims.

ASSOCIATED CONTENT

Supporting Information

The Supporting Information is available free of charge on the ACS Publications website at DOI: 10.1021/acsami.5b04597.

The main synthesized procedure for Fc-NH_2; the possible mechanism and products for PDA-rGO with Fc-NH_2 and cysteine; atomic ratios (%) and N/C ratio of materials determined from XPS spectra; detection ranges and detection limits for DA, UA, HQ, and CC based on the Fc-NH-PDA-rGO/GCE; comparisons of analytical performance of DA, UA, HQ, CC, Pb^{2+}, and Cd^{2+} on electrodes modified with different materials; UV−vis absorption spectra of PDA-rGO with the different reduction times; IR spectra of GOx, PDA-rGO, and GOx-PDA-rGO; CVs and EIS of different material modified electrodes; DPVs of Fc-NH-PDA-rGO/GCE in various concentrations of DA, UA, HQ, and CC; effect of detection conditions on the stripping current of Cd^{2+} and Pb^{2+} at cys-PDA-rGO/GCE; CVs of the GOx-PDA-rGO/GCE in 1 mM glucose at different scan rates (PDF)

AUTHOR INFORMATION

Corresponding Authors

*Tel: +86-731-88872618; fax: +86-731-88872531; E-mail address: liumeilingww@126.com.

*Tel: +86-731-88872618; fax: +86-731-88872531; E-mail address: zhangyy@hunnu.edu.cn.

Notes

The authors declare no competing financial interest.

ACKNOWLEDGMENTS

This work was supported by the National Natural Science Foundation of China (21305042, 21375037, 21275051), the Scientific Research Fund of Hunan Provincial Education Department (14B116, CX2015B165), the Science and Technology Department (14JJ4030, 13JJ2020), the Opening Fund of state key laboratory of Chemo/Biosensing and Chemometrics, Hunan University (2013017), and the Aid Program for Science and Technology Innovative Research Team in Higher Educational Institutions of Hunan Province.

REFERENCES

(1) Lin, D.; Qin, T.; Wang, Y.; Sun, X.; Chen, L. Graphene Oxide Wrapped SERS Tags: Multifunctional Platforms toward Optical Labeling, Photothermal Ablation of Bacteria, and the Monitoring of Killing Effect. *ACS Appl. Mater. Interfaces* **2014**, *6*, 1320−1329.

(2) Abbas, A.; Brimer, A.; Slocik, J. M.; Tian, L.; Naik, R. R.; Singamaneni, S. Multifunctional Analytical Platform on a Paper Strip: Separation, Preconcentration, and Subattomolar Detection. *Anal. Chem.* **2013**, *85*, 3977−3983.

(3) Zhu, C.; Yang, G.; Li, H.; Du, D.; Lin, Y. Electrochemical Sensors and Biosensors Based on Nanomaterials and Nanostructures. *Anal. Chem.* **2015**, *87*, 230−249.

(4) Jin, Y. Multifunctional Compact Hybrid Au Nanoshells: A New Generation of Nanoplasmonic Probes for Biosensing, Imaging, and Controlled Release. *Acc. Chem. Res.* **2014**, *47*, 138−148.

(5) Mieszawska, A. J.; Mulder, W. J. M.; Fayad, Z. A.; Cormode, D. P. Multifunctional Gold Nanoparticles for Diagnosis and Therapy of Disease. *Mol. Pharmaceutics* **2013**, *10*, 831−847.

(6) Chan, H. M.; Li, H. W. Multifunctional Encoded Self-Assembling Protein Nanofibrils as Platform for High-Throughput and Multiplexed Detection of Biomolecules. *Anal. Chem.* **2011**, *83*, 9370−9377.

(7) Tang, J.; Tang, D.; Niessner, R.; Chen, G.; Knopp, D. Magneto-Controlled Graphene Immunosensing Platform for Simultaneous Multiplexed Electrochemical Immunoassay Using Distinguishable Signal Tags. *Anal. Chem.* **2011**, *83*, 5407−5414.

(8) Zhu, Q.; Chai, Y.; Zhuo, Y.; Yuan, R. Ultrasensitive Simultaneous Detection of Four Biomarkers Based on Hybridization Chain Reaction and Biotin-Streptavidin Signal Amplification Strategy. *Biosens. Bioelectron.* **2015**, *68*, 42−48.

(9) Wu, C.; Cheng, Q.; Wu, K. Electrochemical Functionalization of N-Methyl-2-Pyrrolidone-Exfoliated Graphene Nanosheets as Highly Sensitive Analytical Platform for Phenols. *Anal. Chem.* **2015**, *87*, 3294−3299.

(10) Kang, S. M.; Park, S.; Kim, D.; Park, S. Y.; Ruoff, R. S.; Lee, H. Simultaneous Reduction and Surface Functionalization of Graphene Oxide by Mussel-Inspired Chemistry. *Adv. Funct. Mater.* **2011**, *21*, 108−112.

(11) Guo, L.; Liu, Q.; Li, G.; Shi, J.; Liu, J.; Wang, T.; Jiang, G. A Mussel-Inspired Polydopamine Coating as a Versatile Platform for the In Situ Synthesis of Graphene-Based Nanocomposites. *Nanoscale* **2012**, *4*, 5864−5867.

(12) Park, J.; Brust, T. F.; Lee, H. J.; Lee, S. C.; Watts, V. J.; Yeo, Y. Polydopamine-Based Simple and Versatile Surface Modification of Polymeric Nano Drug Carriers. *ACS Nano* **2014**, *8*, 3347−3356.

(13) Sedó, J.; Saiz-Poseu, J.; Busqué, F.; Ruiz-Molina, D. Catechol-Based Biomimetic Functional Materials. *Adv. Mater.* **2013**, *25*, 653−701.

(14) Hu, W.; He, G.; Zhang, H.; Wu, X.; Li, J.; Zhao, Z.; Qiao, Y.; Lu, Z.; Liu, Y.; Li, C. M. Polydopamine-Functionalization of Graphene Oxide to Enable Dual Signal Amplification for Sensitive Surface Plasmon Resonance Imaging Detection of Biomarker. *Anal. Chem.* **2014**, *86*, 4488−4493.

(15) Ryu, J.; Ku, S. H.; Lee, H.; Park, C. B. Mussel-Inspired Polydopamine Coating as a Universal Route to Hydroxyapatite Crystallization. *Adv. Funct. Mater.* **2010**, *20*, 2132−2139.

(16) Zhang, J.; Zhang, W.; Bao, T.; Chen, Z. Mussel-Inspired Polydopamine-Assisted Hydroxyapatite as the Stationary Phase for Capillary Electrochromatography. *Analyst* **2014**, *139*, 242−250.

(17) Ma, Y.-r.; Zhang, X.-l.; Zeng, T.; Cao, D.; Zhou, Z.; Li, W.-h.; Niu, H.; Cai, Y.-q. Polydopamine-Coated Magnetic Nanoparticles for Enrichment and Direct Detection of Small Molecule Pollutants Coupled with MALDI-TOF-MS. *ACS Appl. Mater. Interfaces* **2013**, *5*, 1024−1030.

DOI: 10.1021/acsami.5b04597
ACS Appl. Mater. Interfaces 2015, 7, 17935−17946

(18) Liu, R.; Guo, Y.; Odusote, G.; Qu, F.; Priestley, R. D. Core–Shell Fe_3O_4 Polydopamine Nanoparticles Serve Multipurpose as Drug Carrier, Catalyst Support and Carbon Adsorbent. *ACS Appl. Mater. Interfaces* **2013**, *5*, 9167–9171.
(19) Xie, Y.; Yan, B.; Xu, H.; Chen, J.; Liu, Q.; Deng, Y.; Zeng, H. Highly Regenerable Mussel-Inspired Fe_3O_4@Polydopamine-Ag Core–Shell Microspheres as Catalyst and Adsorbent for Methylene Blue Removal. *ACS Appl. Mater. Interfaces* **2014**, *6*, 8845–8852.
(20) Xia, B. Y.; Wu, H. B.; Yan, Y.; Wang, H. B.; Wang, X. One-Pot Synthesis of Platinum Nanocubes on Reduced Graphene Oxide with Enhanced Electrocatalytic Activity. *Small* **2014**, *10*, 2336–2339.
(21) Xu, L. Q.; Yang, W. J.; Neoh, K.-G.; Kang, E.-T.; Fu, G. D. Dopamine-Induced Reduction and Functionalization of Graphene Oxide Nanosheets. *Macromolecules* **2010**, *43*, 8336–8339.
(22) Fu, Y.; Li, P.; Xie, Q.; Xu, X.; Lei, L.; Chen, C.; Zou, C.; Deng, W.; Yao, S. One-Pot Preparation of Polymer–Enzyme–Metallic Nanoparticle Composite Films for High-Performance Biosensing of Glucose and Galactose. *Adv. Funct. Mater.* **2009**, *19*, 1784–1791.
(23) Lee, H. D.; Shara, M.; Miller, W. M.; Messersmith, P. B. Mussel-Inspired Surface Chemistry for Multifunctional Coatings. *Science* **2007**, *318*, 426–430.
(24) Liu, Y.; Ai, K.; Lu, L. Polydopamine and Its Derivative Materials: Synthesis and Promising Applications in Energy, Environmental, and Biomedical Fields. *Chem. Rev.* **2014**, *114*, 5057–5115.
(25) Choi, I.; Kim, Y. K.; Min, D. H.; Lee, S. W.; Yeo, W. S. On-Demand Electrochemical Activation of the Click Reaction on Self-Assembled Monolayers on Gold Presenting Masked Acetylene Groups. *J. Am. Chem. Soc.* **2011**, *133*, 16718–16721.
(26) Decréau, R. A.; Collman, J. P.; Hosseini, A. Electrochemical Applications. How Click Chemistry Brought Biomimetic Models to the Next Level: Electrocatalysis under Controlled Rate of Electron Transfer. *Chem. Soc. Rev.* **2010**, *39*, 1291–1301.
(27) Camponovo, J.; Ruiz, J.; Cloutet, E.; Astruc, D. New Polyalkynyl Dendrons and Dendrimers: "Click" Chemistry with Azidomethylferrocene and Specific Anion and Cation Electrochemical Sensing Properties of the 1,2,3-Triazole-Containing Dendrimers. *Chem. - Eur. J.* **2009**, *15*, 2990–3002.
(28) Cha, I.; Lee, E. J.; Park, H. S.; Kim, J.-H.; Kim, Y. H.; Song, C. Facile Electrochemical Synthesis of Polydopamine-Incorporated Graphene Oxide/PEDOT Hybrid Thin Films for Pseudocapacitive Behaviors. *Synth. Met.* **2014**, *195*, 162–166.
(29) Liu, M.; Wang, L.; Deng, J.; Chen, Q.; Li, Y.; Zhang, Y.; Li, H.; Yao, S. Highly Sensitive and Selective Dopamine Biosensor Based on a Phenylethynyl Ferrocene/Graphene Nanocomposite Modified Electrode. *Analyst* **2012**, *137*, 4577–4583.
(30) Mazario, E.; Sanchez-Marcos, J.; Menendez, N.; Herrasti, P.; Garcia-Hernandez, M.; Munoz-Bonilla, A. One-Pot Electrochemical Synthesis of Polydopamine Coated Magnetite Nanoparticles. *RSC Adv.* **2014**, *4*, 48353–48361.
(31) Hu, M.; Mi, B. Enabling Graphene Oxide Nanosheets as Water Separation Membranes. *Environ. Sci. Technol.* **2013**, *47*, 3715–3723.
(32) Yamaguchi, H.; Eda, G.; Mattevi, C.; Kim, H. K.; Chhowalla, M. Highly Uniform 300 mm Wafer-Scale Deposition of Single and Multilayered Chemically Derived Graphene Thin Films. *ACS Nano* **2010**, *4*, 524–528.
(33) Hwang, S.-H.; Kang, D.; Ruoff, R. S.; Shin, H. S.; Park, Y.-B. Poly(vinyl alcohol) Reinforced and Toughened with Poly(dopamine)-Treated Graphene Oxide, and Its Use for Humidity Sensing. *ACS Nano* **2014**, *8*, 6739–6747.
(34) Guo, C. X.; Li, C. M. Direct Electron Transfer of Glucose Oxidase and Biosensing of Glucose on Hollow Sphere-Nanostructured Conducting Polymer/Metal Oxide Composite. *Phys. Chem. Chem. Phys.* **2010**, *12*, 12153–12159.
(35) Wu, S.; Ju, H. X.; Liu, Y. Conductive Mesocellular Silica–Carbon Nanocomposite Foams for Immobilization, Direct Electrochemistry, and Biosensing of Proteins. *Adv. Funct. Mater.* **2007**, *17*, 585–592.
(36) Gan, T.; Sun, J.; Huang, K.; Song, L.; Li, Y. A Graphene Oxide–Mesoporous MnO_2 Nanocomposite Modified Glassy Carbon Electrode as a Novel and Efficient Voltammetric Sensor for Simultaneous Determination of Hydroquinone and Catechol. *Sens. Actuators, B* **2013**, *177*, 412–418.
(37) Li, Z.; Chen, L.; He, F.; Bu, L.; Qin, X.; Xie, Q.; Yao, S.; Tu, X.; Luo, X.; Luo, S. Square Wave Anodic Stripping Voltammetric Determination of Cd^{2+} and Pb^{2+} at Bismuth-Film Electrode Modified with Electroreduced Graphene Oxide-Supported Thiolated Thionine. *Talanta* **2014**, *122*, 285–292.
(38) Bao, S.-J.; Li, C. M.; Zang, J.-F.; Cui, X.-Q.; Qiao, Y.; Guo, J. New Nanostructured TiO_2 for Direct Electrochemistry and Glucose Sensor Applications. *Adv. Funct. Mater.* **2008**, *18*, 591–599.

DOI: 10.1021/acsami.5b04597
ACS Appl. Mater. Interfaces 2015, 7, 17935–17946